Portable Microwave Test Packages for Beam-Waveguide Antenna Performance Evaluations

Tom Y. Otoshi, *Senior Member, IEEE,* Scott R. Stewart, *Member, IEEE,* and Manuel M. Franco, *Member, IEEE*

***Abstract*—Portable microwave test packages used to evaluate a new 34-m-diameter beam-waveguide (BWG) antenna are described. The experimental methodology involved transporting test packages to different focal points of the BWG system and making noise temperature, antenna efficiency, and holography measurements. Comparisons of data measured at the different focal points enabled determinations of performance degradations caused by various mirrors in the BWG system. It is shown that, due to remarkable stabilities and accuracies of radiometric data obtained through the use of the microwave test packages, degradations caused by the BWG system were successfully determined.**

I. Introduction

A NEW 34-m-diameter beam waveguide (BWG) antenna has been built at the NASA/JPL Goldstone, California tracking facility. A unique experimental technique was used to evaluate this antenna. The methodology involved the use of portable test packages transported to different focal-point locations of the BWG system. Focal points f1, f2, and f3 are depicted in Fig. 2 of a companion article in this issue [1]. Focal point f1 is the Cassegrain focal point near the main reflector vertex. An intermediate focal point f2 lies above the azimuth track, and focal point f3 is the final BWG focal point located in a subterranean pedestal room. Degradations caused by the BWG system mirrors and shrouds were determined from comparisons made of values measured at the different focal points.

The complete experimental program used three different microwave test packages and tested the antenna at three frequency bands: *X*-band (8.45 GHz), *Ku*-band (12 GHz), and *Ka*-band (32 GHz). With the exception of holography data obtained at 12 GHz, all microwave performance data on the BWG antenna were based on noise-temperature measurement data obtained through the use of the test-packages and a total-power radiometer system.

Manuscript received May 28, 1991; revised October 11, 1991. The research described in this paper was carried out by the Jet Propulsion Laboratory, California Institute of Technology, under a contract with the National Aeronautics and Space Administration.

T. Y. Otoshi and M. M. Franco are with the Jet Propulsion Laboratory, California Institute of Technology, 4800 Oak Grove Drive, Pasadena, CA 91109.

S. R. Stewart is with PRC, Pasadena, CA 91107.

IEEE Log Number 9107469.

This article will present brief descriptions of the test packages, test procedures, installations, noise-temperature measurement method, and a summary of operating system-noise temperatures measured at various focal points. More detailed descriptions of the various test packages, tabulated data and plots for operating system-noise temperatures for different observation periods, and radiometer system performance may be found in [2]–[6]. The results of *X*- and *Ka*-band antenna efficiency tests at f1 and f3 are presented in a companion article in this issue [7]. *Ku*-band holography tests at f1 were successfully performed and the results are also presented in this issue [8].

II. Test-Package Descriptions

Fig. 1 is a photograph of the *X*-, *Ku*-, and *Ka*-band (partially assembled) test packages under test at JPL before shipment to Deep Space Station 13 (DSS 13). In their final configurations, both the *X*- and *Ka*-band test packages contain many of the familiar Cassegrain cone components such as a 22-dBi horn, polarizer, round-to-rectangular transition, waveguide switch, waveguide ambient load, directional coupler, cryogenically cooled low-noise amplifier, noise diode assembly, and downconverter (receiver). Fig. 2 is a block diagram of the *X*-band test package. The block diagram for the *Ka*-band test package is nearly identical, with the exceptions that (1) the *Ka*-band test package does not have the two circular rotary joints, and (2) the *Ka*-band downconverter local-oscillator frequency is derived from a 32-GHz Gunn Oscillator.

After amplifications by the high-electron-mobility transistors (HEMTs), the *X*- and *Ka*-band microwave signals were downconverted to, respectively, 350-MHz and 60-MHz IF and sent via coaxial cable to a total-power radiometer system located in the pedestal room. Block diagrams of the downconverter and noise-box assemblies for the *X*- and *Ka*-band test packages are given, respectively, in [2], [3], and [4].

III. Test Configurations and Test Procedure

Figs. 3 and 4 show the mounting structure (removable after test) and the *X*-band test package installed at the Cassegrain focal point f1. Fig. 5 shows the *X*-band test pack-

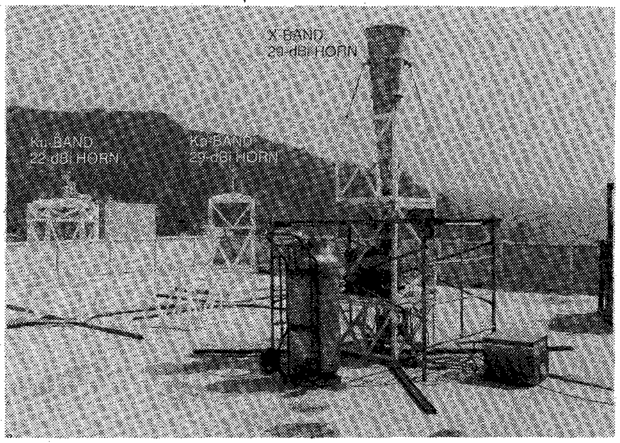

Fig. 1. *X*-band test package under test at JPL. The *Ku*- and *Ka*-band (partially assembled) test packages are also shown.

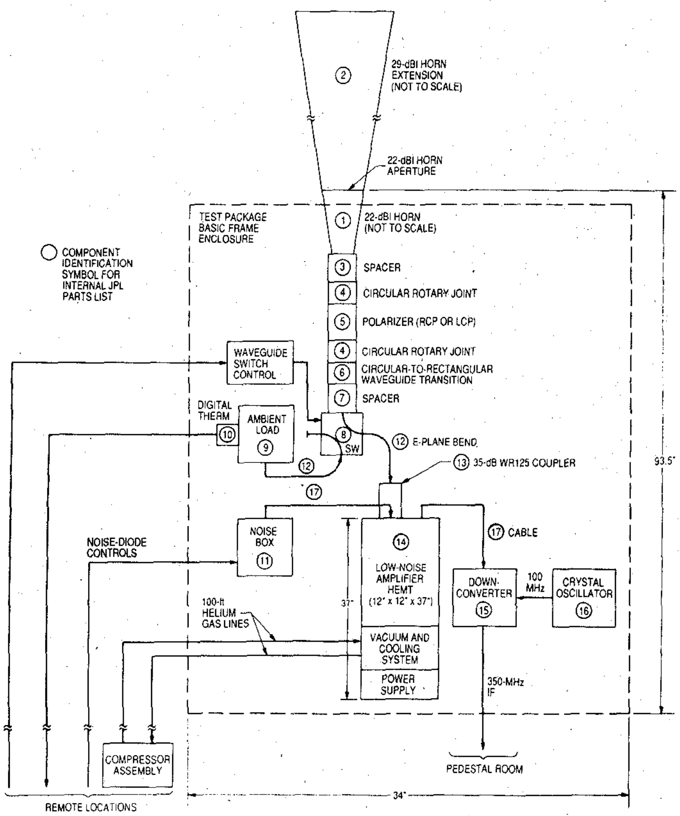

Fig. 2. The *X*-band test package system.

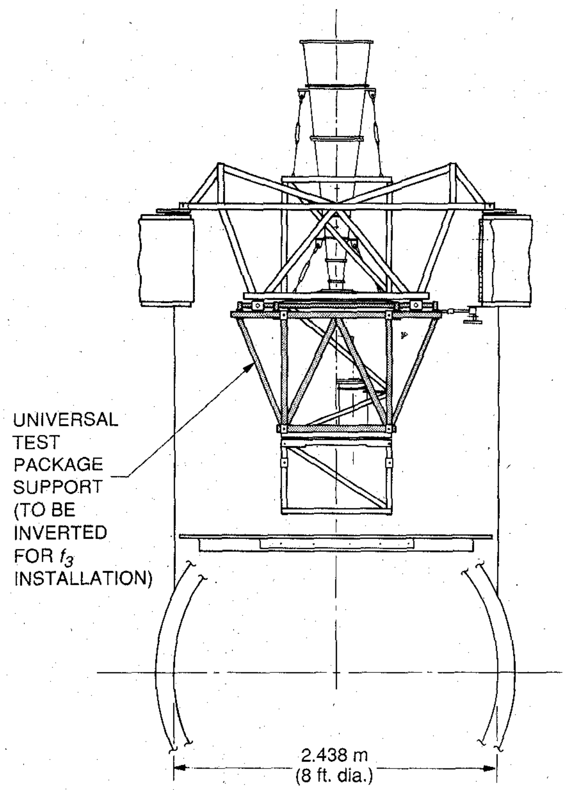

Fig. 3. Overall view of the mounting structure and the *X*-band test package at f1 in the 29-dBi horn configuration.

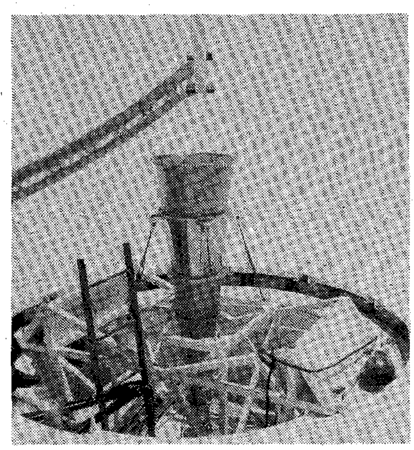

Fig. 4. Partial view of the *X*-band 29-dBi horn test package and mounting structure installed at the Cassegrain focal point f1.

age installed on a universal three-axis adjustable mounting table at the f3 pedestal-room location. The mounting structure at f1 and mounting table at f3 allow any of the three test packages to be easily interchanged. At f1, the test packages are in a 29-dBi horn configuration, while at f3, the *X*- and *Ka*-band test packages are in 22-dBi and 23-dBi horn configurations, respectively.

To test the BWG antenna at f1 and f3, it was required that each test package be convertible between 22-dBi (or 23-dBi) and 29-dBi horn configurations. The conversions were accomplished through the use of horn extensions of the same taper going from the 22- (or 23-) to the 29-dBi horn aperture diameters appropriate for the horn design frequencies. Table I shows the phase centers for the installations at f1 and f3. The phase centers were computed for the horn design frequencies and not for the actual test frequencies, which were 8.45 GHz for *X*-band, 11.7 and 12.2 GHz for *Ku*-band, and 32 GHz for *Ka*-band. The small differences in phase centers that resulted from the small differences between test and design frequencies were not critical. The mounting assemblies (Figs. 4 and 5) were designed such that upon installation of a particular test package at the desired antenna focal-point location, the phase center of the horn coincided with the focal point.

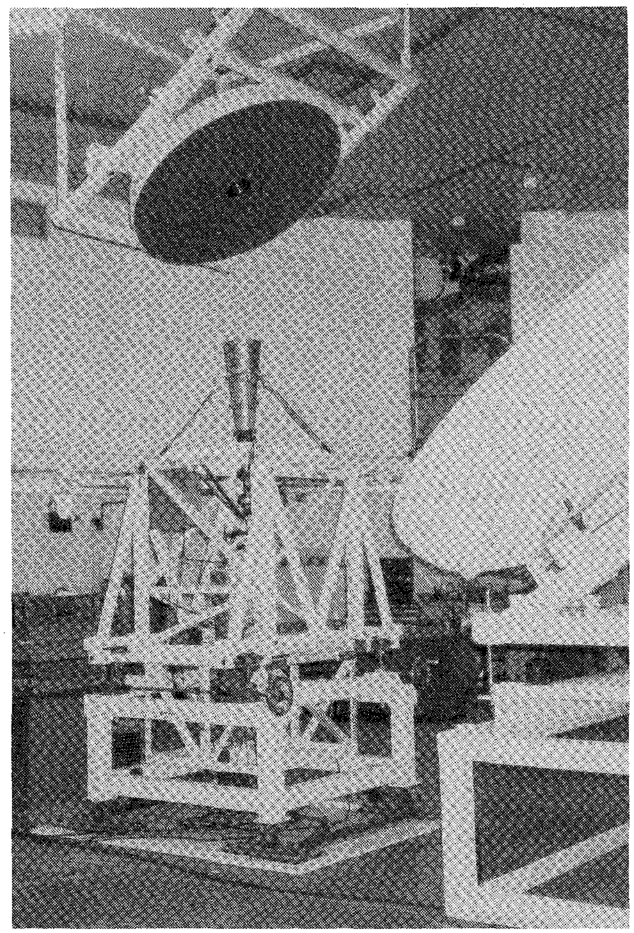

Fig. 5. *X*-band 22-dBi horn test package and mounting table installed in the pedestal room focal point f3.

TABLE I
TEST-PACKAGE HORN PHASE CENTERS

Band	Horn Design Frequency, GHz	Phase Center Location Relative to Horn Aperture, in.	Gain, dBi
	Phase Centers at f1 and f2 for 29-dBi Horn Configurations		
X	8.420	−46.45 (f1) −49.38 (f2)	29.79
Ku	12.198	−32.97 (f1)	29.98
Ka	32.000	−11.80 (f1) −11.41 (f2)	29.93
	Phase Centers at f3 for 22-dBi Horn Configurations		
X	8.420	−3.34	22.34
Ku	12.198	−2.45	22.55
Ka	32.000	−1.03	22.88

Where necessary, any deviation of phase center from the focal-point location was compensated through adjustments of the subreflector Z-focus position for f1 measurements, and adjustments of the test-package mounting table (in the pedestal room) for f3 measurements.

The test procedure required clear sky reference measurements first with the test package located on the ground with the horn pointed at zenith. Noise-temperature and antenna-efficiency measurements were then made as functions of antenna pointing angles with the appropriate portable test package installed at the Cassegrain focal point f1. The test package was then transported to other focal points of the BWG mirror system, and measurements were again made. Degradations caused by the BWG mirror sys-

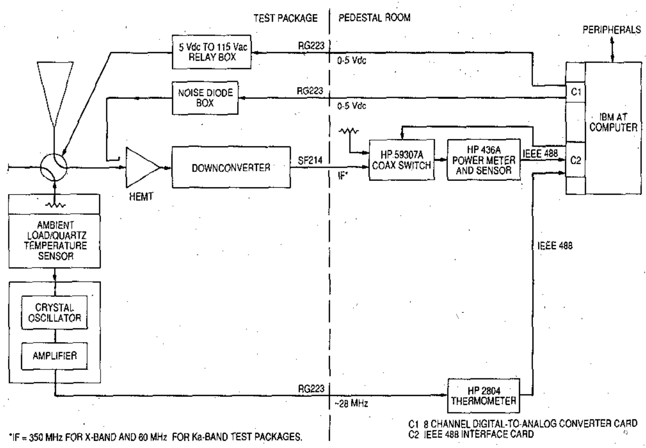

Fig. 6. The interface between the X- or Ka-band test package and the total-power radiometer system.

TABLE II
DEFINITIONS OF SYMBOLS AND ABBREVIATIONS

Symbol	Definition
T'_{cb}	Effective noise temperature contribution to T_{op} from the cosmic background radiation, K. This value is a function of frequency and will differ from the actual cosmic background noise temperature of 2.7 K. $$T'_{cb} = T_{cb}\left[\frac{x}{\exp(x) - 1}\right], \text{ where } x = hf/(kT_{cb})$$
T_{cb}	Cosmic background radiation noise temperature, nominally 2.7 K
h	Planck's constant
f	Frequency, Hz
k	Boltzmann Constant
T_{atm}	Atmospheric noise temperature, K
T_{wg}	Noise temperature due to waveguide loss between the horn aperture and the input flange of the HEMT, K
T_{hemt}	Effective noise temperature of the HEMT as defined at the input flange of the HEMT, K
T_{fup}	Effective noise temperature of the followup receiver (downconverter + cables + power meter, etc.) as defined at the input flange of the HEMT, K
T_{op}	Operating system-noise temperature as defined at the input flange of the HEMT, K
T_s	Source noise temperature, K
L_{wg}	Loss factor for waveguide between the horn aperture and the input flange of the HEMT, power ratio >1
L_{atm}	Loss factor of the atmosphere, power ratio >1

tem were determined by taking the differences of operating noise temperature and antenna gain* values measured at the various focal points.

IV. Noise-Temperature Measurement Method

Fig. 6 shows the automated radiometer system used with the test packages for making noise temperature measurements. Measurements of the IF power output from the downconverter are made on an HP 436A power meter. The power-meter readings are sent to an IBM-AT computer that averages 15 readings per second and converts the values into noise temperatures. Best accuracy is achieved if the system operates well below the saturation point in the linear region. Only two points are then needed to establish a power-reading versus noise-temperature linear calibration curve. The first point corresponds to the power-meter reading when the power meter is zeroed, and the second required point corresponds to the power-meter reading when the waveguide switch is in the ambient-load position. Operating noise temperatures are computed from equations found in [9]. The method is based on knowing the ambient load physical temperature and the effective noise temperature of the HEMT (from lab or field tests). It is assumed that the HEMT noise temperature does not change with time or test-package motions.

The basis of the real-time corrections for receiver system gain changes is precise knowledge of the current ambient-load physical temperature. The ambient-load physical temperature is measured at $\pm 0.01\,^{\circ}$C resolution through the aid of a digital readout thermometer embedded in the ambient-load reference termination. Nonlinearity of the system is determined from power-meter readings when the noise diode signal is injected into the

*Antenna gain is determined from the efficiency, aperture area, and frequency, and expressed in dB.

TABLE III
SUMMARY OF X-BAND ZENITH OPERATING SYSTEM-NOISE TEMPERATURES AT DSS 13 FROM JUNE 10, 1990–FEB. 2, 1991

Configuration	Observation Dates	Grand Average[a] T_{op}, K	Peak Deviations from Grand Average, K
Ground	06/10/90, 01/21/91, 01/26/91	22.7	+0.3 −0.3
f1	10/04/90	25.9	—
f2	01/12/91, 01/12/91 (two different time periods, same day)	30.1	+0.2 −0.3
f3	11/06/90, 11/09/90	34.2	+0.1 −0.2
After Mirrors and Ellipsoid Realigned on Dec. 18, 1990			
f3	01/31/91, 02/02/91	34.8	+0.1 −0.1

[a]For each observation period, the measured T_{op} was normalized to a Goldstone average clear zenith X-band atmosphere of 2.17 K for DSS 13 and an X-band test package waveguide noise temperature T_{wg} = 4.69 K as based on a standard waveguide physical temperature of 20°C (see [3] for methodology).

TABLE IV
SUMMARY OF Ka-BAND ZENITH OPERATING SYSTEM-NOISE TEMPERATURES AT DSS 13 FROM OCT. 12, 1990–JAN. 31, 1991

Configuration	Observation Dates	Grand Average[a] T_{op}, K	Peak Deviations from Grand Average, K
Ground	10/12/90, 11/09/90, 01/19/91, 01/31/91	84.7	+1.6 −1.7
f1	10/13/90, 10/14/90, 01/11/91	91.8	+0.4 −0.6
f2	01/16/91, 01/17/91	97.0	+0.4 −0.4
f3	11/10/90, 12/18/90	102.4	+0.1 −0.0
After Mirrors and Ellipsoid Realigned on Dec. 18, 1990			
f3	01/23/91, 01/25/91, 01/30/91	98.6[b]	+0.8 −0.7

[a]For each observation period, the measured T_{op} was normalized to a Goldstone average clear zenith Ka-band atmosphere of 7.02 K for DSS 13 and a Ka-band test package waveguide loss noise temperature T_{wg} = 17.67 K as based on a standard waveguide physical temperature of 20°C (see [5] for methodology).
[b]This number cannot be compared with the above f2 value. It is probable that the new f2 value is also lower after the mirror realignment, but a measurement was not made.

HEMT and the switch is first in the "antenna" position and then in the "ambient-load" position. The test packages are designed to have nonlinearity errors of less than 1%. Nonlinearity errors are kept small by use of appropriate padding, filters, and amplifiers and mixers that do not saturate at the expected input levels.

All measurements and data processing are performed automatically by the computer. The system is recalibrated periodically or instantaneously as desired by the experimenter. Correction factors for system nonlinearity [10] and gain changes are computed from the last system calibration. An option for displaying corrected noise temperatures in real-time is available. Most options are executed by means of a single keystroke command from the user.

V. NOISE-TEMPERATURE MEASUREMENT RESULTS

Noise-temperature symbols are used in an equation and the tables that follow. For the reader's convenience, the symbols are defined in Table II.

Measurements with the test packages on the ground and at various focal points of the BWG antenna covered a span of several months. Tables III and IV show the final grand

TABLE V
DIFFERENTIAL ZENITH OPERATING SYSTEM-NOISE TEMPERATURES FOR VARIOUS TEST CONFIGURATIONS

	Delta T_{op}, K	
Configurations Differenced	*X*-band	*Ka*-band
f1 − ground	3.2	7.1
f2 − f1	4.2	5.2
f3 − f1	8.3	10.6
After Mirrors and Ellipsoid Realigned on Dec. 18, 1990		
f3 − f1	8.9	6.8

See Tables III and IV for f1, f2, and f3 values.

TABLE VI
X- AND *Ka*-BAND TEST-PACKAGE PERFORMANCE CHARACTERISTICS

Parameter	*X*-band	*Ka*-band
Receive polarization	RCP, LCP or fixed linear	RCP or LCP (if reconfigured)
Receive frequencies	8.4–8.5 GHz (predetermined by inherited DSN downconverter)	31.865–32.085 GHz from lab tests
T_{op} on ground at DSS-13, zenith clear sky	<23 K	85 K actual[a]
Measured T_{op} resolution for the above T_{op} value, $\tau = 1$ s 100-MHz BW	<0.02 K	<0.06 K
Gain stability over 0 to 40°C ambient temperature range	<0.3 dB p-p, <0.1 dB typical, <0.05 dB/h Downconverter in an ovenized box	<0.2 dB p-p, <0.05 dB/h Downconverter has thermoelectric temperature control
Total calibrated nonlinearity error	<1%	<2%
Radio source temp (T_s) measurement accuracy (a delta measurement)	± [0.02 + 0.010 × T_s] K for $2 < T_s < 10$ K	± [0.06 + 0.020 × T_s] K for $2 < T_s < 10$ K
Overall T_{op} measurement accuracy,[b] K $10 < T_{op} < 150$ K	<0.4 K p-p	<0.8 K p-p

[a]A major part of the total is due to 56.6 K from the HEMT and 17.7 K from waveguide losses.
[b]Based on error analysis, calibration errors, and estimated mismatch errors.

averages of zenith operating system-noise temperatures at *X*-band and *Ka*-band, respectively. Corrections have been made for weather and waveguide ambient temperatures. All values have been normalized for Goldstone average clear *X*- and *Ka*-band atmospheres and a waveguide ambient temperature of 20°C. More details on the methodology for data reduction may be found in [3] and [5].

When the test package is on the ground, the general expression for the operating system-noise temperature is

$$T_{op} = T'_{cb}/(L_{atm}L_{wg}) + T_{atm}/L_{wg} + T_{wg} + T_{hemt} + T_{fup} \quad (1)$$

Under standard conditions at 8.45 GHz, the component values are $T'_{cb} = 2.5$ K, $T_{atm} = 2.17$ K, $T_{wg} = 4.69$ K, $T_{hemt} = 13$ K, and $T_{fup} = 0.4$ K; $L_{atm} = 1.00814$ (corresponding to 0.0352 dB) and $L_{wg} = 1.0163$ (corresponding to 0.07 dB). Substitutions of the values into (1) results in a predicted T_{op} of 22.7 K, which agrees with the measured ground value of 22.7 K shown in Table III. An estimate of the one standard deviation of the tabulated measured value for each configuration shown on Table III is ±0.3 K.

Under standard conditions at 32.0 GHz, the component values are $T'_{cb} = 2.0$ K, $T_{atm} = 7.02$ K, $T_{wg} = 17.67$ K, $T_{hemt} = 56.6$ K, and $T_{fup} = 1.8$ K; $L_{atm} = 1.02683$ (corresponding to 0.1150 dB) and $L_{wg} = 1.06414$ (corresponding to 0.27 dB). Substitutions of the values into (1) results in a predicted T_{op} of 84.5 K, which agrees closely with the measured ground value of 84.7 K shown in Table IV. An estimate of the one standard deviation of the tabulated measured value for each configuration shown in Table IV is ±0.7 K.

One of the primary goals of the experimental project was to determine degradations caused by the BWG mirror system. The results given in Table V show that this goal was achieved. The difference between f1 and ground operating system-noise temperatures reveals the amount of degradation caused by spillover of the subreflector and main reflector, scattering from the tripod legs, and leakage through gaps between panels and perforations in the main reflector surfaces. The difference between f2 and f1 operating system-noise temperatures provides information on the upper four mirrors (two flat mirrors and two paraboloids), while the difference between f3 and f1 provides data on the upper four mirrors, the ellipsoid, and a flat mirror above the feedhorn.

Table VI lists the microwave performance characteristics of the *X*- and *Ka*-band test packages. The characteristics are based on error analyses and several months of field data [2]–[5]. The test packages performed better than expected with regard to the linearity and short and long-term gain stability. All test packages were designed to be mechanically stable, and, in the field, their stabilities were verified by the fact that the microwave performance characteristics were maintained whenever any of the test packages was mounted at f1 and the antenna was tipped from zenith to the 5-deg elevation angle. The test packages proved to be rugged in hostile environments and continued to work well even after repeated moves between f1, f2, f3, and the ground.

The outstanding electrical and mechanical characteristics of the *X*- and *Ka*-band test packages (and radiometer system) enabled the packages to be used for BWG system diagnostic purposes as well as for efficiency [7], pointing-error, subreflector defocusing-curve, and tipping-curve measurements. Tipping-curve and subreflector test data for different focal points of the BWG antenna at *X*- and *Ka*-band may be found in [3] and [5].

VI. Concluding Remarks

The goal of measuring BWG systems degradation through the use of portable test packages has been achieved at *X*- and *Ka*-band. Tests using a *Ku*-band (12-GHz) test package for holography purposes were similarly successful [8]. From the tests results presented in this report, it can be stated that the test packages and radiometer system are state-of-the-art antenna performance evaluation instruments. To the authors' knowledge, the test-package method is the first known experimental method for determining the degradations caused by the BWG system of a large antenna.

Acknowledgment

Many persons in various technical divisions at the Jet Propulsion Laboratory have furnished subassemblies and contributed to the successful development of the test packages. In particular the authors thank technical contributions made by D. Bathker on the test-package concept and L. Skjerve and C. T. Stelzried on the radiometer calibrations and computer program. The superb mechanical designs of the test package and associated antenna and pedestal room mounting assemblies are credited to S. Katow, V. Lobb, R. Bryant, and D. Ohashi, all of the Ground Antenna and Facilities Engineering Section at JPL. The support provided by DSS 13 personnel during all phases of testing is gratefully acknowledged. Project manager G. Wood, Systems Engineer D. L. Brunn, and Test Coordinator M. Britcliffe contributed to the successful completion of this project.

References

[1] D. A. Bathker, W. Veruttipong, T. Y. Otoshi, and P. W. Cramer, Jr., "Beam-waveguide antenna performance predictions with comparisons to experimental results," *IEEE Trans. Microwave Theory Tech.*, vol. 40, no. 6, June 1992.

[2] T. Y. Otoshi, S. R. Stewart, and M. M. Franco, "A portable X-band front-end test package for beam-waveguide antenna performance evaluation, Part 1: design and ground tests," *TDA Progress Report 42-103*, Jet Propulsion Laboratory, Pasadena, CA, pp. 135–150, Nov. 15, 1990.

[3] —, "A portable X-band front-end test package for beam-waveguide antenna performance evaluation, Part II: tests on the antenna," *TDA Progress Report 42-105*, Jet Propulsion Laboratory, Pasadena, CA, pp. 54–68, May 15, 1991.

[4] —, "A portable Ka-band front-end test package for beam-waveguide antenna performance evaluation, Part I: design and ground tests," *TDA Progress Report 42-106*, Jet Propulsion Laboratory, Pasadena, CA, pp. 249–265, Aug. 15, 1991.

[5] —, "A portable Ka-band front-end test package for beam-waveguide antenna performance evaluation. Part II: tests on the antenna," *TDA Progress Report 42-106*, Jet Propulsion Laboratory, Pasadena, CA, pp. 266–282, Aug. 15, 1991.

[6] —, "A portable Ku-band front-end test package for beam-waveguide antenna performance evaluation," *TDA Progress Report 42-107*, Jet Propulsion Laboratory, Pasadena, CA, Nov. 15, 1991.

[7] S. D. Slobin, T. Y. Otoshi, M. J. Britcliffe, L. S. Alvarez, S. R. Stewart, and M. M. Franco, "Efficiency measurement techniques for calibration of a prototype 34-m-diameter beam-waveguide antenna at 8.45 and 32 GHz," *IEEE Trans. Microwave Theory Tech.*, vol. 40, no. 6, June 1992.

[8] D. J. Rochblatt and B. L. Seidel, "Microwave antenna holography," *IEEE Trans. Microwave Theory Tech.*, vol. 40, no. 6, June 1992.

[9] C. T. Stelzried, "Operating noise temperature calibrations of low-noise receiving systems," *Microwave J.*, vol. 14, no. 6, pp. 41–46, 48, June 1971.

[10] —, "Non-linearity in measurement systems: evaluation method and application to microwave radiometers," *TDA Progress Report 42-91*, Jet Propulsion Laboratory, Pasadena, CA, pp. 57–61, Nov. 15, 1987.

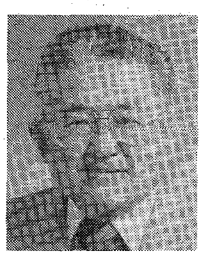

Tom Y. Otoshi (S'53–M'56–SM'74) was born in Seattle, WA on September 4, 1931. He received the B.S.E.E. and M.S.E.E. degrees from the University of Washington, Seattle in 1954 and 1957, respectively.

From 1956 to 1961, he was a Member of the Technical Staff at Hughes Aircraft Company, Culver City, CA where he was involved in guided-missile checkout equipment development, microwave primary standards, radome and antenna research, and the development of microwave components. In 1961, he joined the Communications Elements Research Section of the Jet Propulsion Laboratory (JPL), California Institute of Technology, Pasadena, CA, as a Senior Engineer and was promoted to Member of the Technical Staff in 1974. He has been engaged in the analysis and calibration of low-noise antenna systems, radio science projects, group delay and ranging measurement projects, antenna multipath studies, VLBI, and the development of precision frequency stability measurement techniques for deep space tracking stations. More recently, he has been involved in the development of a dual-passband low-noise dichroic plate, and also in beam-waveguide antenna evaluations involving noise temperature, antenna efficiency, and frequency stability measurements.

Mr. Otoshi is a member of Tau Beta Pi and Sigma Xi.

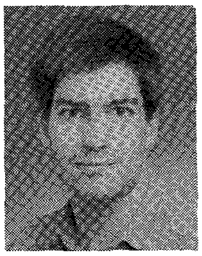

Scott R. Stewart (S'87–M'90) was born in Lompoc, CA on September 28, 1965. He received the B.S. degree in electronic engineering from the California Polytechnic State University in San Luis Obispo, CA, in 1989.

In 1987, he joined the Engineering Technology Group of PRC, Inc., Pasadena, CA, which supports the Ground Antennas and Facilities Section of the Jet Propulsion Laboratory (JPL), California Institute of Technology, Pasadena, CA. He has been involved in the calibration of low-noise microwave receiver systems, and in the evaluations of noise temperature and antenna efficiency performance of beam-waveguide antennas.

Manuel M. Franco (M'91) was born in Jerez, Zacatecas, Mexico February 20, 1950, and received the AA degree in Electronics Technology in 1973 and another AA degree in Computer Technology in 1974. He has completed short microwave engineering courses at George Washington University in Washington D.C. and is near completion of his B.S. degree in electronics from California State Polytechnic University at Pomona, California.

He has 22 years experience with California Institute of Technology, Jet Propulsion Laboratory, in Pasadena, and has helped to develop a wide spectrum of low-noise microwave receiver and instrumentation systems for spacecraft tracking, radiometry, and radio astronomy. In addition to his continued involvement with design, development, and field operation of prototype microwave systems, he has focussed his efforts on the Ground Observatory Program, which utilizes the large Deep Space Network (DSN) antennas and low-noise receivers for special radio astronomy and other science observations. His designs are presently in operation at all three DSN complexes—Australia, Spain, and the United States.